4.1 Introduction

Refractories are the backbone of any high-temperature manufacturing unit. These are generally produced in combination or alone from alumina, silica, magnesia, zirconia, chromia, etc., due to their stability and chemical inertness at high temperatures [123,124]. Among them, the alumina-silica group of refractories are widely used and, based on their physical and chemical nature, classified as fireclay refractories and high alumina refractories [46]. Fireclay refractories are formed from natural clay (silica-rich), which can withstand a temperature above the PCE (pyrometric cone equivalent) value of 19 without disintegrating, deforming, cracking, softening, or melting. These refractories are mainly composed of kaolinite clay minerals ($Al_2O_3 \cdot 2SiO_2 \cdot 2H_2O$), and the typical composition of fire clay bricks is SiO_2 (< 78%) and Al_2O_3 (< 44%). As a result, the most common uses of these classes of refractories are in power generation blast furnaces, chimney linings, boilers, glass tank furnaces, and pottery kilns. Fireclay is also used to make pouring refractories such as nozzles, sleeves, stoppers, and tuyers [123–125].

In thermal power plants, energy has been produced by burning pulverized coal. In the course of combustion, carbon and volatile matter are burned off along with the impurities such as clay, quartz, feldspar, shale, etc. These impurities remain in the suspension and are later condensed into fly ash in low temperatures, which is recognized as an environmental pollutant and hazardous material [59]. A vast quantity (750 million tonnes) of fly ash has been generated every year worldwide, and in India, 196.44 million tonnes of fly ash was generated in 2017-18 [8,9]. The fly ash comprises

toxic trace constituents, and therefore expensive precautions are needed for dumping the fly ash. Fly ash is very much hazardous and can cause land and water pollution, which is unacceptable both from economic and environmental points of view [101,126]. Therefore, a constant interest is growing among scientists to establish appropriate practices where fly ash can be used efficiently. To date various researchers have investigated the utilization of fly ash in different fields, such as building bricks [127–129], cement [130], concrete [59,131], geopolymer [132], glass-ceramics [133], and lightweight aggregate for the construction industry [134,135].

Nowadays, researchers have investigated the application of fly ash in the shaped and unshaped refractory. Ardha et al. investigated that fly ash could be used as an alumina and silica source to prepare acid-based castables after demagnetization. They have found that the refractoriness of the demagnetized fly ash was 1305 °C which was increased to 1465 °C when mixed with grog [40]. Consequently, Anja et al. report that mechanically activated coal fly ash can be used as microfiller in manufacturing refractory bauxite shotcrete, which reduces structural void and pores that can be used up to 1400 °C [103]. Gonzalez et al. used 65 %fly ash to make insulating fire bricks where porosity was 71-80%, and CCS was found to be in the range of 2.83-5.05 MPa [67]. Hassan et al. have shown that coal fly ash can be incorporated in alumino-silicate clay for the application of furnace linings. They found that 25 wt.% coal fly ash can effectively increase the TSR (thermal shock resistance) and CCS of the refractory linings [136]. On the other hand, Sukkae et al. have found that the addition of calcia rich (25%) coal fly ash into fireclay can effectively reduce linear shrinkage and thermal conductivity along with the mechanical properties of the refractories body [102]. So, therefore it is essential to make a thorough study to understand the role of fly ash and

ball clay on the properties of fireclay refractory produced at high temperature. The present study was undertaken to use the lignite fly ash of an Indian origin for the fabrication of fireclay refractories to meet up the industrial requirements. The successful application will lead us to the utilization of waste product lignite fly ash that needs special care for redemption and effective use of this fly ash as a refractory raw material. These two different roles can cater to the Indian refractory industry in terms of cost-saving and environmental issues.

The main objective of this investigation is the utilization of Indian-origin lignite fly ash to develop fireclay refractory bricks, which can be a value-added product.

The formulations of five different batches (C-1to C-5) by incorporating lignite fly ash (≤ 250 μm) and ball clay (≤ 75 μm) are shown in **Table 4.1**. The fabrication process is discussed in **Chapter 3**.

Table 4.1 Batch composition of different formulations.

Samples	Fly Ash (wt.%)	Ball Clay (wt.%)
C-1	90	10
C-2	80	20
C-3	70	30
C-4	60	40
C-5	50	50

4.2 Results and discussions

The chemical composition of as received lignite fly ash and ball clay is shown in **Table 4.2**. The lignite fly ash powder consists primarily of SiO_2 and Al_2O_3, which is summed up about 91%.

Table 4.2 Chemical composition of fly ash and ball clay.

Compounds (wt.%)	Lignite fly ash	Ball clay
SiO_2	67.10	53.80
Al_2O_3	23.99	30.21
Fe_2O_3	5.50	1.25
TiO_2	0.96	1.30
CaO	0.95	1.20
MgO	0.27	0.45
Na_2O	0.59	0.30
K_2O	0.23	0.80
LOI	--	10.69

Fig. 4.1 (b) shows the XRD pattern of lignite fly ash powder. The primary identified crystalline phase was quartz (SiO_2), whereas the minor phase was mullite ($3Al_2O_3.2SiO_2$). However, the surface morphology of the fly ash powder is shown in **Fig. 4.2 (a)**, which shows that particles are almost glassy, porous, flaky, and irregular in shape.

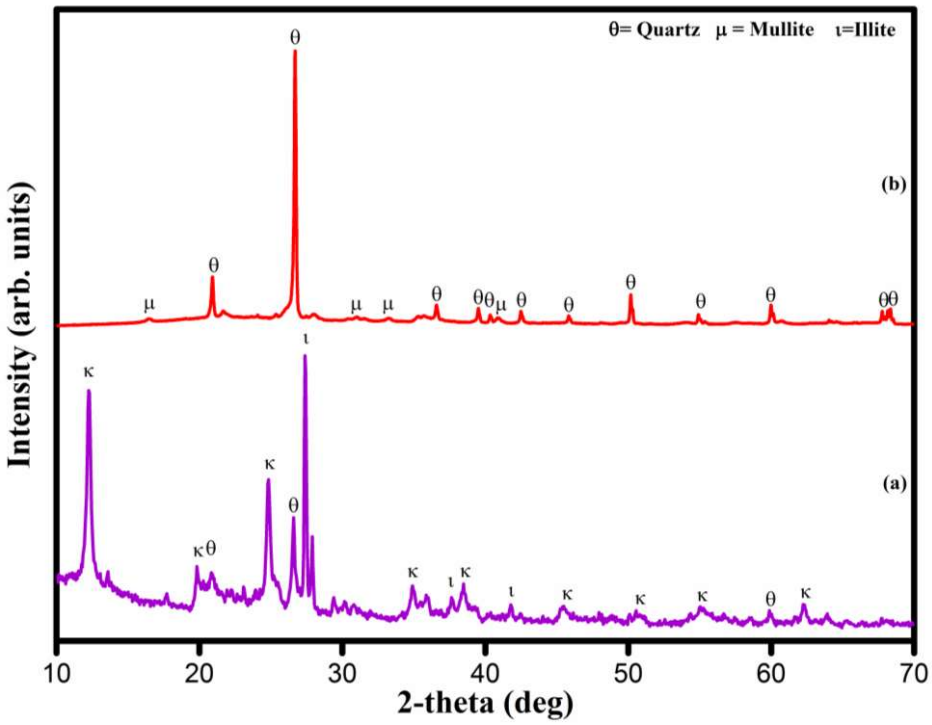

Fig. 4.1: XRD curves of (a) ball clay and (b) fly ash.

On the other hand, **Table 4.2** also shows the ball clay chemical composition. The ball clay powder comprises silica (SiO_2) and alumina (Al_2O_3), which corresponds to approximately 84%. The high loss of ignition (10.69%) is due to the presence of organic matter, hydroxides, and clay minerals. The amount of Na_2O and K_2O is low, indicating that carbonate is also low. Subsequently, the XRD pattern of ball clay powder is shown in **Fig. 4.1 (a)**. It can be observed that ball clay powder contains the main mineralogical phase of kaolinite, illite, quartz, and minor hematite phase. **Fig. 4.2 (b)** exhibits the microstructure of ball clay powder. The clay particles are irregular and sheet-like structure. The ball clay is mainly used to impart plasticity to the fabricated body. On the other hand, the ball clay is also a source of alumina, which is an important refractory oxide.

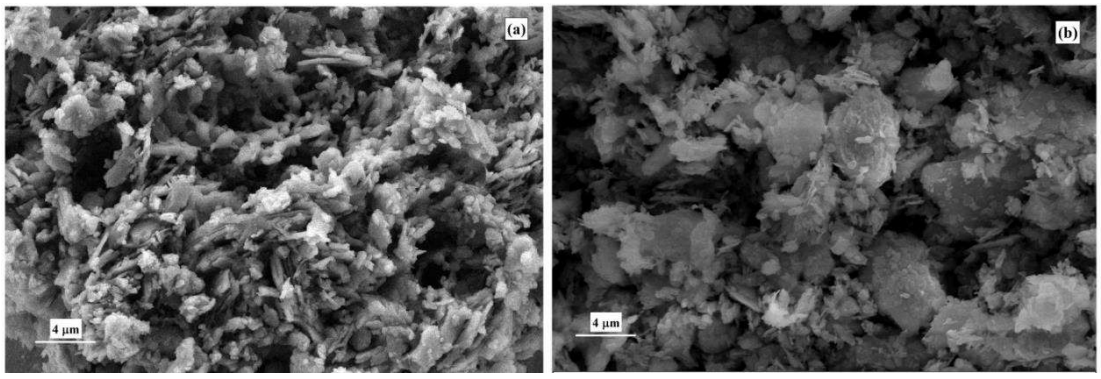

Fig. 4.2: SEM images of (a) lignite fly ash and (b) clay.

The development that takes place during firing is decomposition, phase transformation, and sintering. The intensity and development of the sintering process are affected by decomposition and phase transitions [137]. Differential thermal analysis of the raw mixtures (C-1 to C-5) was performed from 27 to 1100 °C at a heating rate of 10 °C/min in an air atmosphere shown in **Fig. 4.3**. In the DTA curves

(**Fig. 4.3**), it can be observed that it has two distinct endothermic peaks denoted by dash-dot line (1 and 2) and a clear exothermic peak marked by dash-dot line 3. The first endothermic peak represents the vaporization of surface water at about 111 °C, and the second endothermic peak (reaction) shows the removal of structural water (converted to meta-kaoline) as well as phase transformation of quartz (α-β) [38,132,138–141]. These transformations can be shown by following reactions (1) and (2), respectively.

$$Al_2O_3 \cdot 2SiO_2 \cdot 2H_2O \xrightarrow{545-565\ ^\circ C\ (endo)} Al_2O_3 \cdot 2SiO_2 \quad (4.1)$$

$$\alpha\text{-Quartz } (SiO_2) \xrightarrow{545-565\ ^\circ C\ (exo)} \beta\text{-Quartz } (SiO_2) \quad (4.2)$$

The exothermic hump between dash-dot lines 1 and 2 is due to the burning of organic materials in raw mixtures [140].

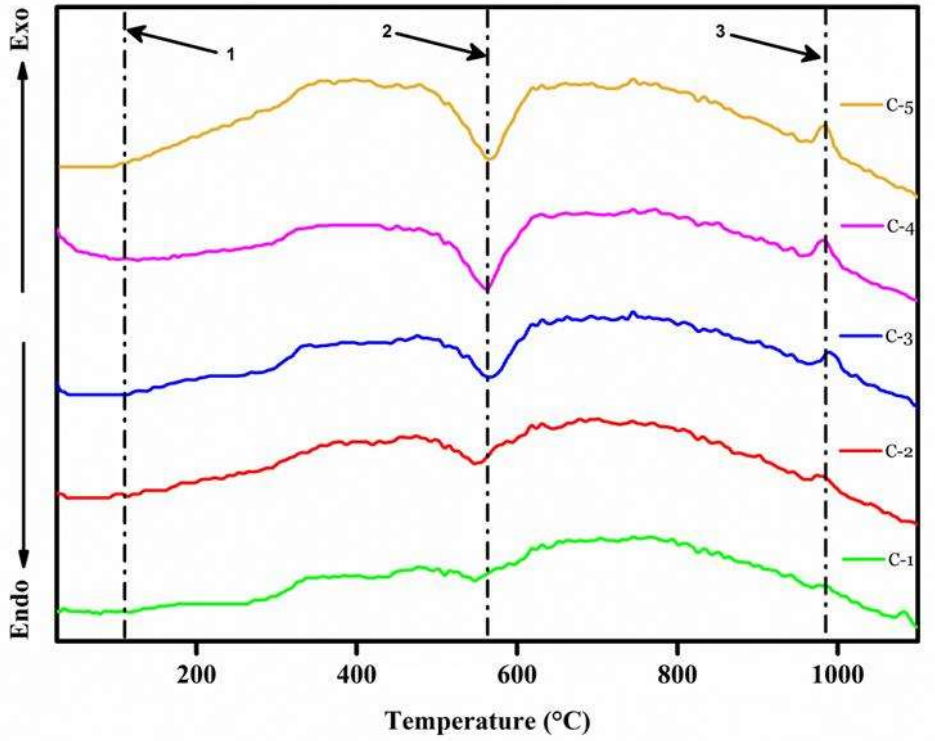

Fig. 4.3: Differential thermal analysis curves of different samples (C-1, C-2, C-3,

C-4 and C-5).

Consequently, the third exothermic peak (dash-dot line 3) indicates the transformation of metakaolin to Al-Si spinel (major), weakly crystalline mullite, and amorphous SiO_2 (glass). The exothermic peak is shown by the following reaction (3).

$$Al_2O_3 \cdot 2SiO_2 \xrightarrow{983\ ^\circ C\ (exo)} \begin{cases} \text{A1} - \text{Si spinel (major)} \\ \text{weakly crystalline mullite} \\ \text{amorphous } SiO_2 \end{cases} \quad (4.3)$$

Subsequently, the exothermic hump between dash-dot lines 2 and 3 may be due to crystal phase formation and structural changes [140,142]. As observed from the DTA curve, the increasing the clay content from C-1 to C-5 and decreasing fly ash content, the exothermic peak intensity also increases, possibly the more crystallization of mullite phase [143]. This mullite phase will increase the strength of the fireclay refractory [142].

The chemical composition of the fired sample of different formulations is shown in **Table 4.3**. The results indicate that the fired sample's minimum SiO_2 and Al_2O_3 content is 66.30 wt.% (C-5) and 21.50 wt.% (C-1), respectively. On the other hand, the fired sample's maximum SiO_2 and Al_2O_3 content is 71.70 wt.% (C-1) and 25.54 wt.% (C-5), respectively. Formulation C-5 consists of the lowest amount of Fe_2O_3 (1.18 wt.%) followed by formulation C-4, which has a value of 1.66 wt.%. The formulation C-1 has the highest Fe_2O_3 content (3.00 wt.%) while formulationC-2 and C-3 have moderate values (2.52 and 2.14 wt.%), respectively. The iron oxide content determines the properties of the fireclay refractory, so low Fe_2O_3 is desirable.

Table 4.3 Chemical composition of different fired samples.

Formula (wt.%)	C-1	C-2	C-3	C-4	C-5
SiO_2	71.70	70.35	69.00	67.65	66.30
Al_2O_3	21.50	22.49	23.47	24.55	25.54
Fe_2O_3	3.00	2.52	2.14	1.66	1.18
CaO	1.33	1.56	1.78	2.01	2.23
TiO_2	0.70	1.02	1.23	1.44	1.76
Na_2O	0.78	0.79	0.80	0.81	0.82
K_2O	0.38	0.47	0.55	0.63	0.72
MgO	0.34	0.43	0.52	0.61	0.70
Cr_2O_3	0.01	0.01	0.01	0.01	0.01
ZrO_2	0.05	0.07	0.09	0.11	0.13
P_2O_5	0.03	0.04	0.05	0.06	0.07
BaO	0.04	0.05	0.05	0.05	0.06
SrO	0.02	0.03	0.03	0.03	0.04

X-ray diffractogram of different formulations sintered at 1000 °C, 1100 °C, and 1200 °C is shown in **Fig. 4.4 (a) (b)** and **(c)**, respectively. It is evident from **Fig. 4.4 (a)** that the major crystalline phase is quartz and the minor phases are mullite ($3Al_2O_3.2\ SiO_2$) and cristobalite (SiO_2), which support the DTA results (**Fig. 4.3**) [137]. In the case of **Fig. 4.4 (b)**, the result shows that the major crystalline phases are quartz, mullite ($3Al_2O_3.2\ SiO_2$), and cristobalite (SiO_2). As we can see that the intensity of the crystalline phases increases with increasing clay content (decreasing fly ash). The results are more prominent in **Fig. 4.4 (c)** because the samples are fired at 1200 °C, enhancing the mullite phase formation. The mullite and cristobalite are refractory phases that provide strength to the fired products [45,144,145].

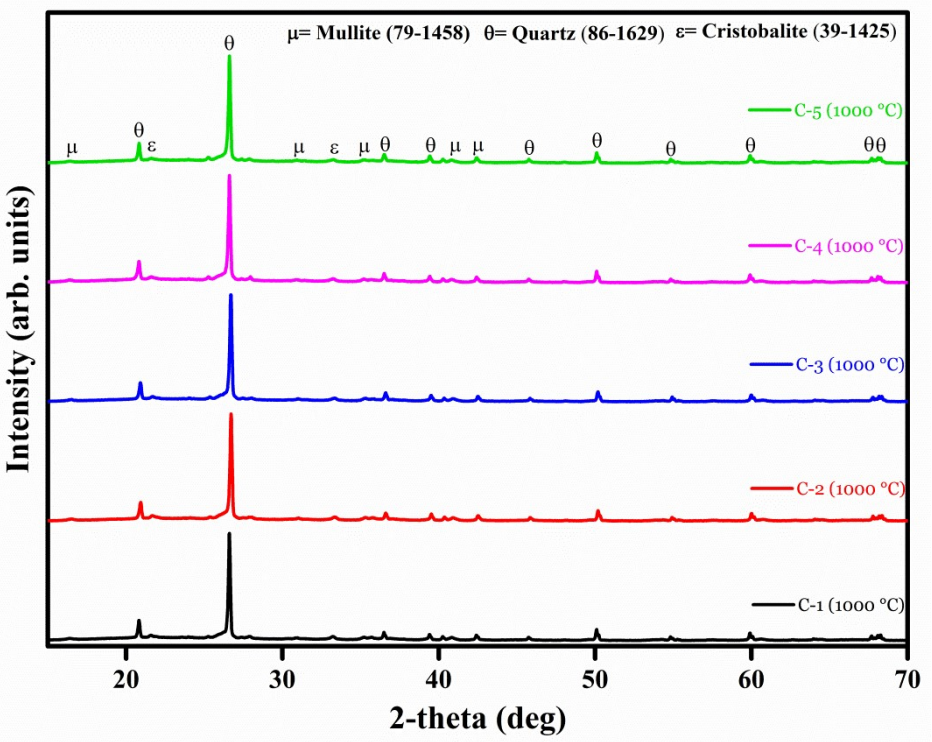

Fig. 4.4 (a): X-Ray diffractogram of different samples fired at 1000 °C.

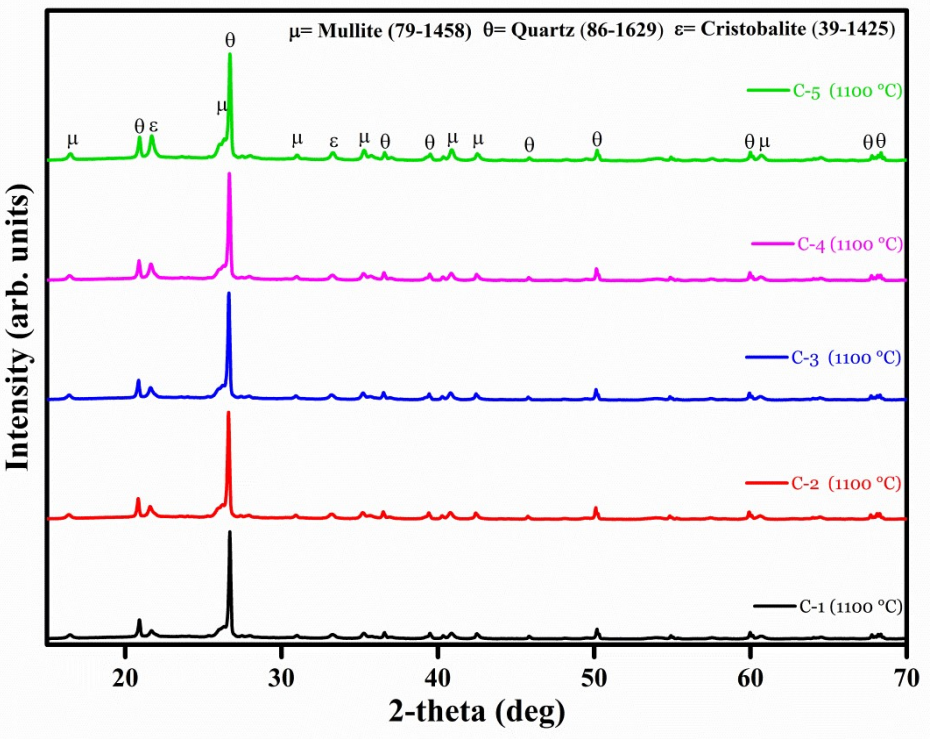

Fig. 4.4 (b): X-Ray diffractogram of different samples fired at 1100 °C.

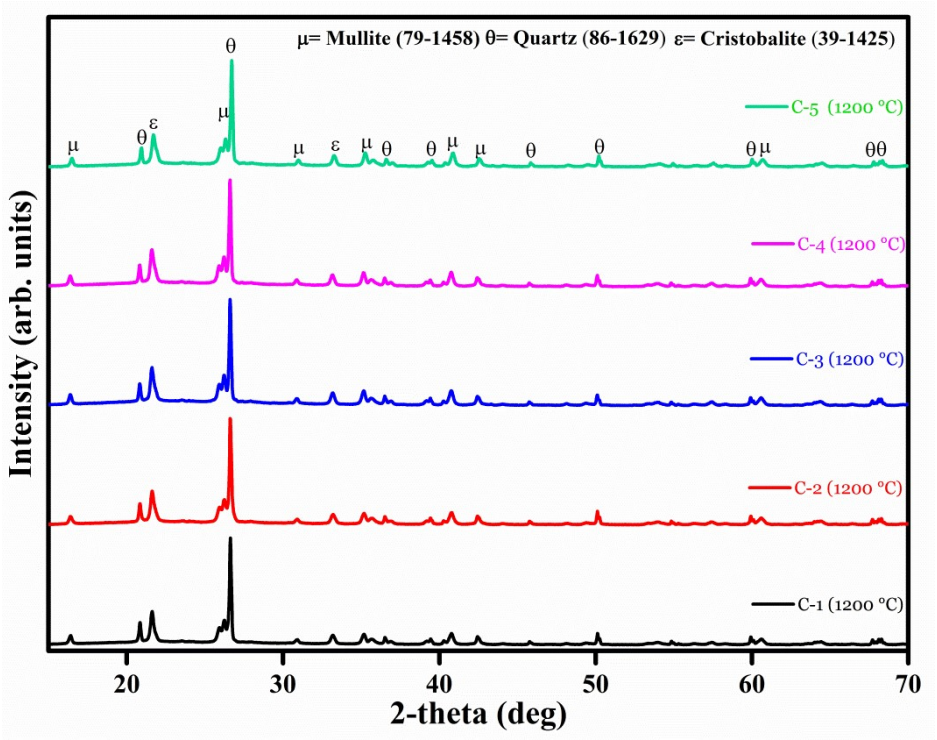

Fig. 4.4 (c): X-Ray diffractogram of different samples fired at 1200 °C.

The total linear shrinkage of the different fired samples as a function of composition is shown in **Fig.4.5**. It can be observed from Fig.6 that upon increasing the firing temperature and clay content up to 50 wt.% (decreasing fly ash content up to 50 wt.%) the linear shrinkage of the fired samples increases. Linear shrinkage can be used as a measurement of densification tool. The shrinkage values are 0.05-0.98 % at 1000 °C for the samples of C-1 to C-5, whereas these values are 1.62-3.27 % (C-1 to C-5) at 1100 °C. At higher firing temperatures (1200 °C), the shrinkage values drastically increase which were found to be 2.85, 3.66, 4.25, 5.03 and 5.38 % for C-1, C-2, C-3, C-4 and C-5, respectively. The low shrinkage values at 1000 °C for all the formulations are possibly due to evaporation of surface water, dehydroxylation of clay, and organic matter burnout. The high shrinkage value of C-5 (5.38 %) compared to C-1 (2.85) at 1200 °C because of removal of large number of pores and thereby better

densification. The primary reason of densification is the higher viscous flow due to the fluxing action as the C-5 formulation has 50% clay and 50% fly ash [137]. However, the total linear shrinkage for all the formulations is significantly less, i.e., 0.05-5.38 %, which may be 50-90% lignite fly ash content [102,136].

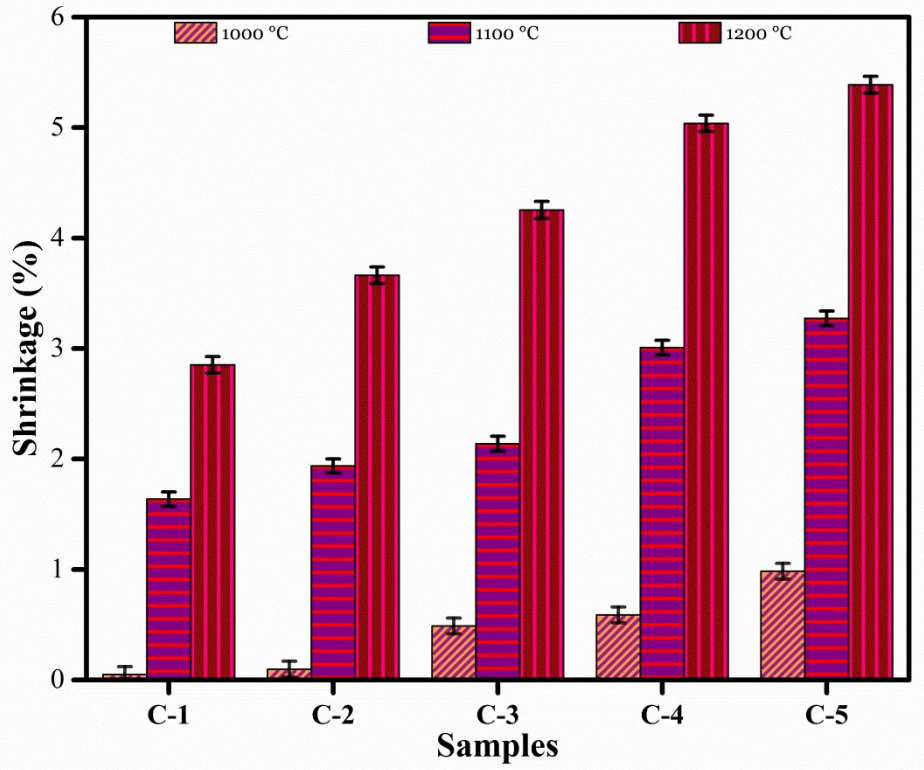

Fig. 4.5: The linear shrinkage of different samples fired at different temperatures.

The bulk density (BD) of fireclay refractory bricks is an important parameter in determining their performance. **Fig. 4.6** exhibits the bulk density of different compositions and sintering temperatures. It can be seen that as the temperature increases, the density of the bricks also increases. Bulk density values of the different formulations (C-1 to C-5) varied between 1.70 to 2.10 gm/cc due to the change in proportion of fly ash to clay and sintering temperatures. The temperature increment causes particle's densification, melting of low temperature phases and generating a

dense amorphous phase, which flows into the pores and deposits. The bulk density of fired samples was linearly proportional to temperature and the amount of clay added to the mixture in this study. The bulk density of fired pieces decreased as fly ash content increased. This behaviour was associated with some pores created by the combustion of organic matter and unburnt carbon previously presented in fly ash. However, the highest density (2.10 gm/cc) achieved at 1200 °C for sample C-5 met the ASTM standard as well as a commercially available product [145–147].

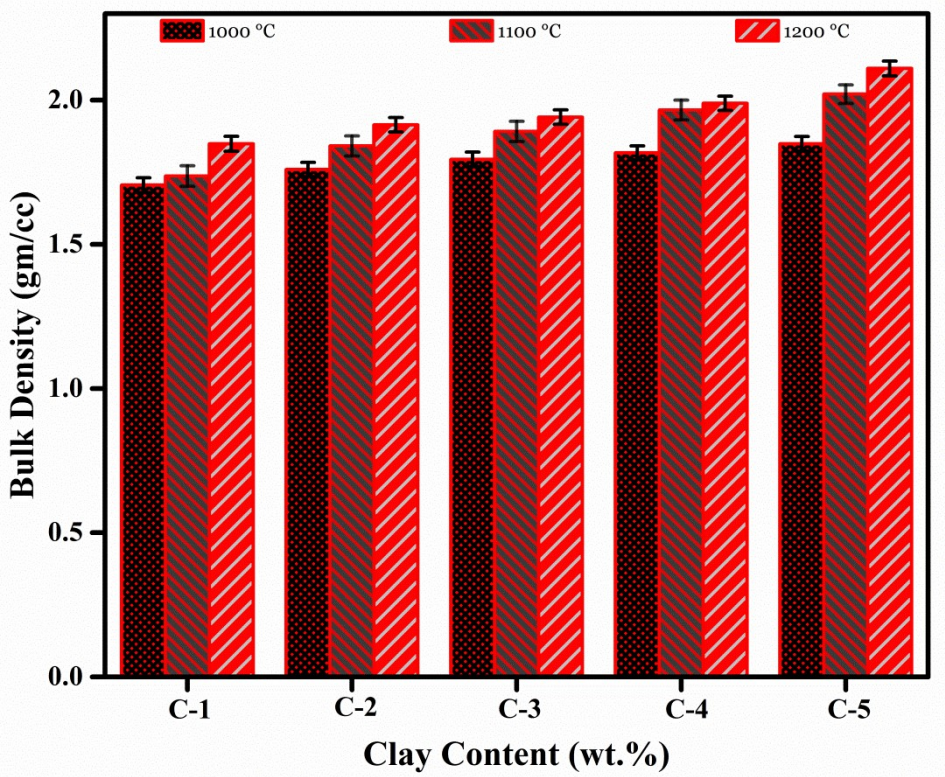

Fig. 4.6: Bulk Density (BD) of different samples as function of composition and firing temperature.

The apparent porosity (AP) values of the fired samples are presented in **Fig. 4.7** as a function of clay content in the composition. It is also observed that the porosity varied between 16% and 36.77 %. The highest porosity was achieved in C-1 (1000

°C), whereas the lowest porosity in C-5 (1200 °C). C-1 to C-5 firing temperature at 1000 °C, the porosity decreases from 36.77 to 31.96%, whereas firing temperature at 1200 °C, the porosity reduces from 27.90 to 15.00% [145]. The reduction in porosity may be due to densification, removal of the pore by vitreous phase, and conversion of meta-kaolin to mullite and glass. So, the size of the fired sample reduces and increases the mechanical properties [148,149].

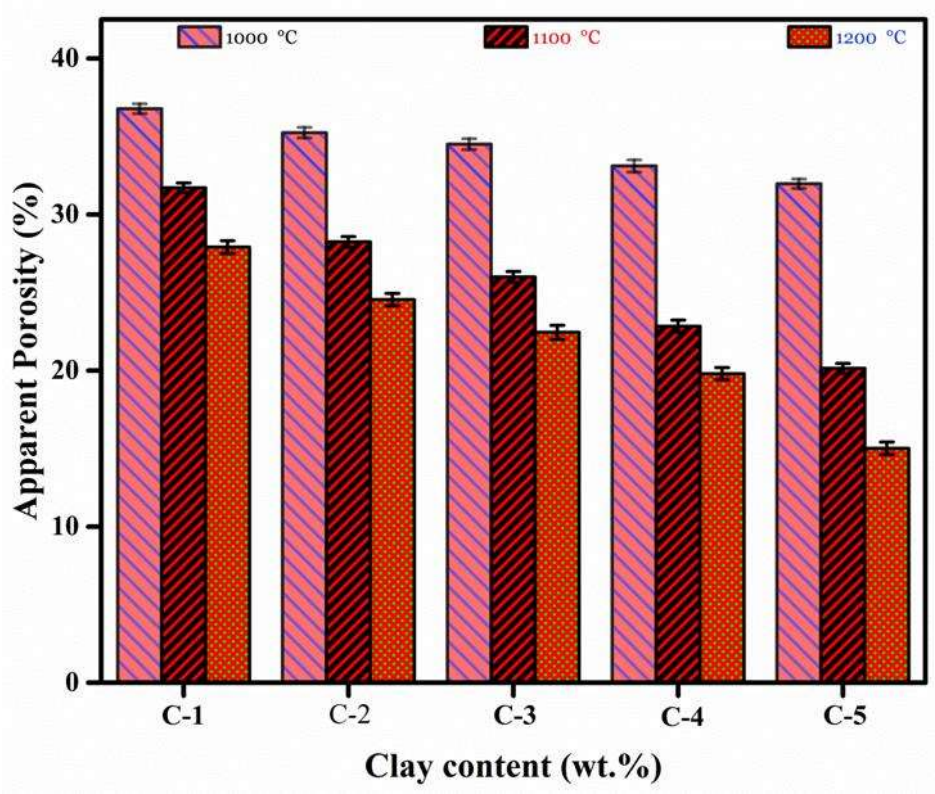

Fig. 4.7: Apparent Porosity (AP) of different samples as function of composition and firing temperature.

The effect of variation in composition on the CCS at various firing temperatures has been shown in **Fig. 4.8**. The results exhibit that CCS values increased strongly with increasing firing temperatures. At 1000 °C, the CCS values are 9.41, 12.01, 16.66, 23.96, and 28.99 for the composition of C-1 to C-5, respectively.

Consequently, at 1200 °C, the CCS values are 13.21, 20.95, 29.03, 42.49, and 52.50

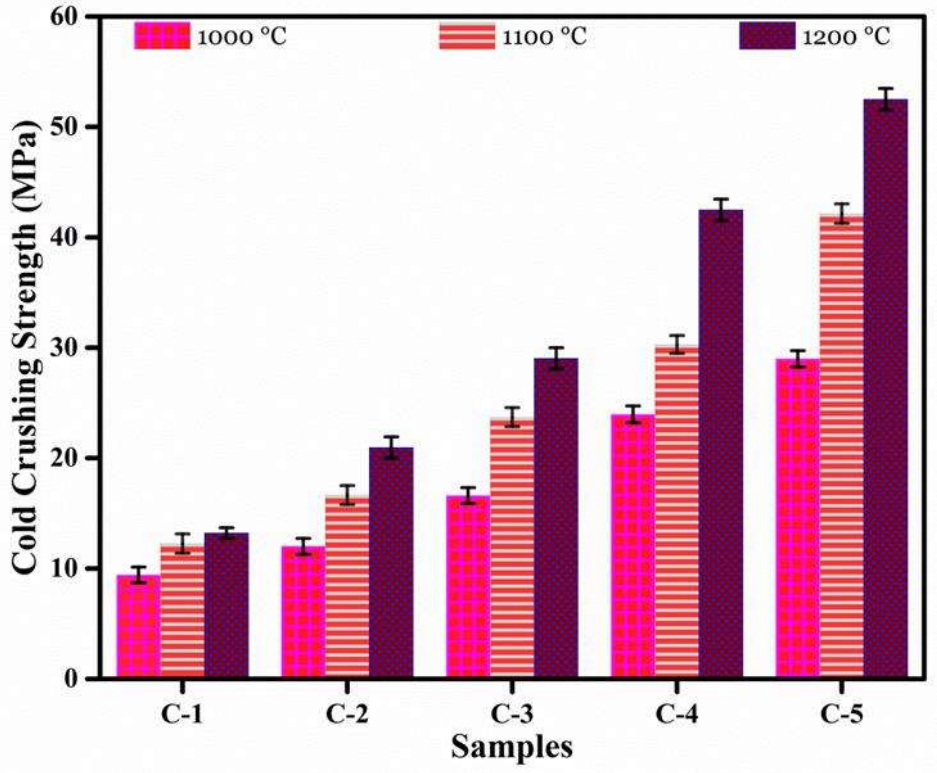

Fig. 4.8: Cold crushing strength (CCS) of different samples fired at different temperatures.

MPa for the composition of C-1 to C-5, respectively. The fly ash, clay content, and phase composition affect the cold crushing strengths of the sintered samples. The highest CCS value was achieved, estimated at 52.50MPa at 1200 °C for C-5 samples that matched ASTM standard and commercially available product [145–147]. The fluxing agents improved the CCS value of the fired samples by densification and also increasing the formation of cristobalite and mullite, resulting in strength [45,124,129,148–150].

Fig.4.9 shows the effect compositions on the cold modulus of rupture (CMOR) at various firing temperatures. The cold modulus of rupture increases linearly with increasing clay content (up to 50 wt.%) and firing temperature. The maximum CMOR

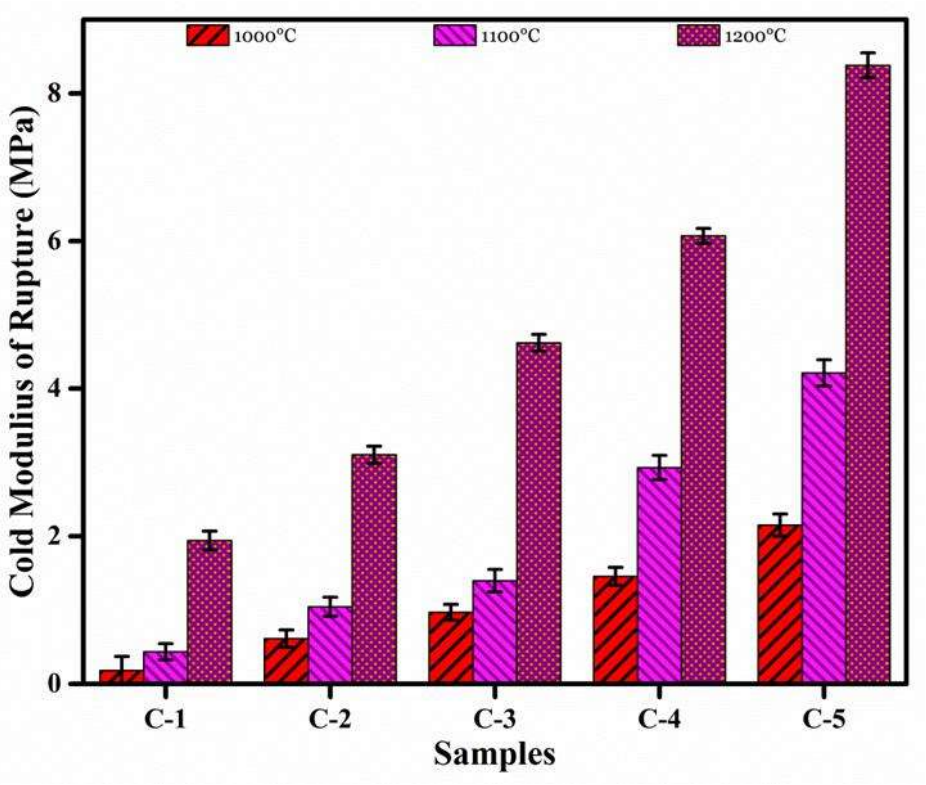

Fig. 4.9: Cold modulus of rupture (CMOR) of different samples fired at different temperatures.

value is achieved at about 8.38 MPa at 50 wt.% ball clay addition (C-5) fired at 1200 °C, which meets the ASTM standard and commercial product for fireclay refractories [145–147]. However, pore reduced the strength of the fired samples, which acts as a stress concentration for cracks. The increase in ball clay addition (up to 50 wt.%) decreases the porosity and increases the interlocking matrix phase in the fired sample, so enhancing in strength [124,150].

The thermal conductivity of the different samples sintered at 1000, 1100, and 1200 °C measured at 600 and 1000 °Care illustrated in **Fig. 10 (a), (b),** and **(c)**, respectively. The results indicate that as increasing temperature and clay content (up to 50 wt.%), the thermal conductivity of the fired sample decreases. The highest achieved thermal conductivity value measuring at 1000 °C is estimated to be 0.90

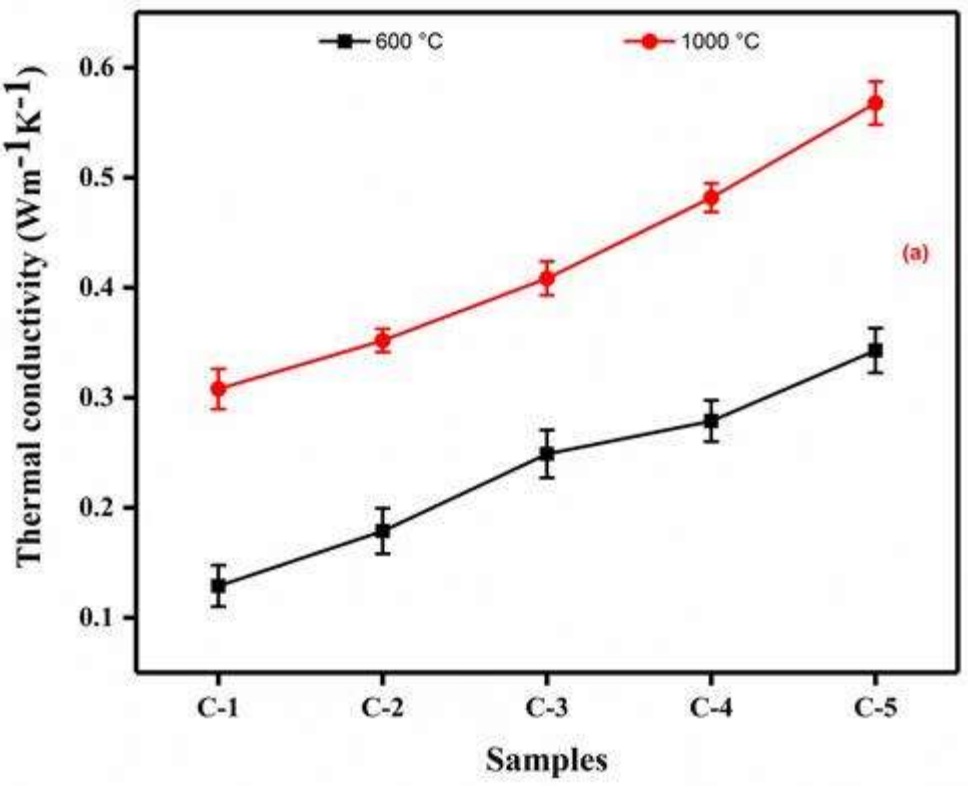

Fig. 4.10 (a): Thermal conductivity of different samples fired at 1000 °C.

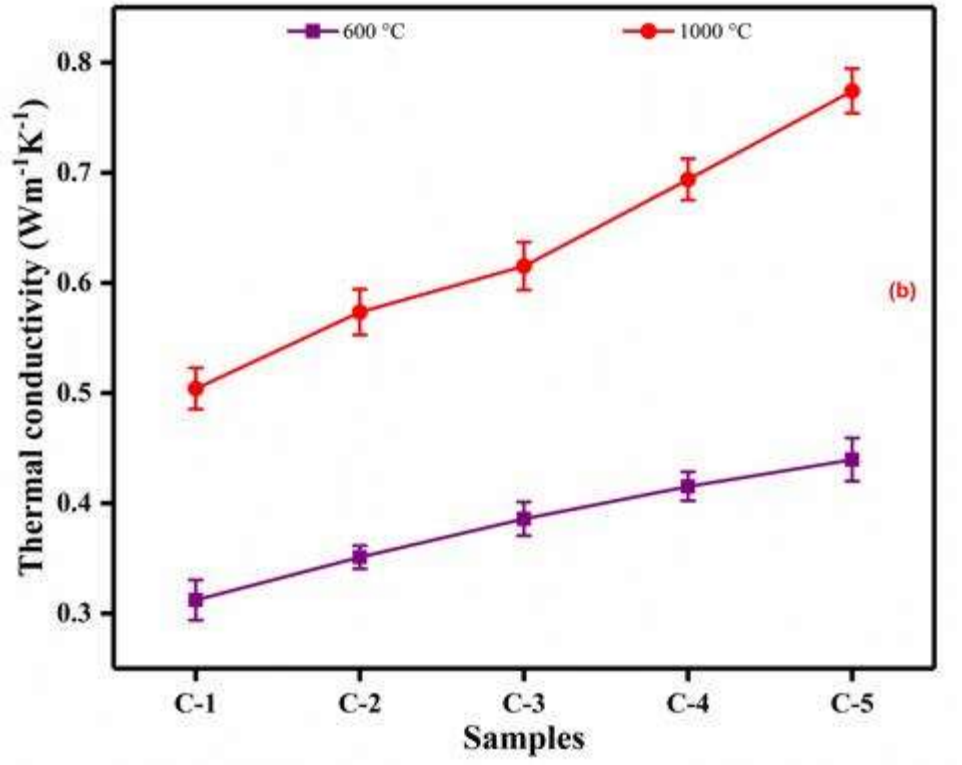

Fig. 4.10 (b): Thermal conductivity of different samples fired at 1100 °C.

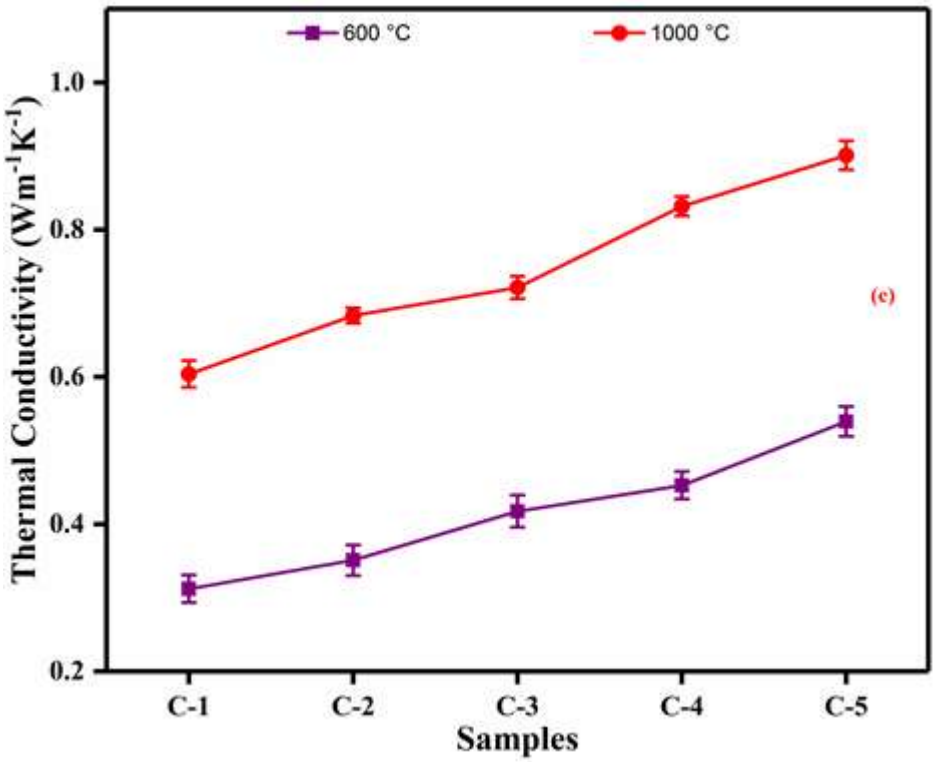

Fig. 4.10 (c): Thermal conductivity of different samples fired at 1200 °C.

W/mK (C-5 at 1200 °C), and the lowest acquired value measuring at 600 °C is 0.13 W/mK (C-1). This could be explained by the low thermal conductivity of formulation C-1has low density and high porosity compared to formulation C-5. The variation in thermal conductivity may be due to the size and shape of pores, microstructure, and various phases present, such as crystalline, amorphous, and glassy phases resulting during sintering of the samples [151–154]. However, all the thermal conductivity values support the standards [145–147].

Fig. 4.11 (a), (b), (c), (d), and **Fig. 4.13(a)** show the SEM images of the different formulations fired at 1200 °C. The mullite and cristobalite embryos started to form gradually at 983 °C, confirmed by XRD. The amorphous glassy phase starts forming after 1000 °C, and the liquid phase also generally increases as the firing temperature and clay content increases. This liquid phase help to grow mullite grain

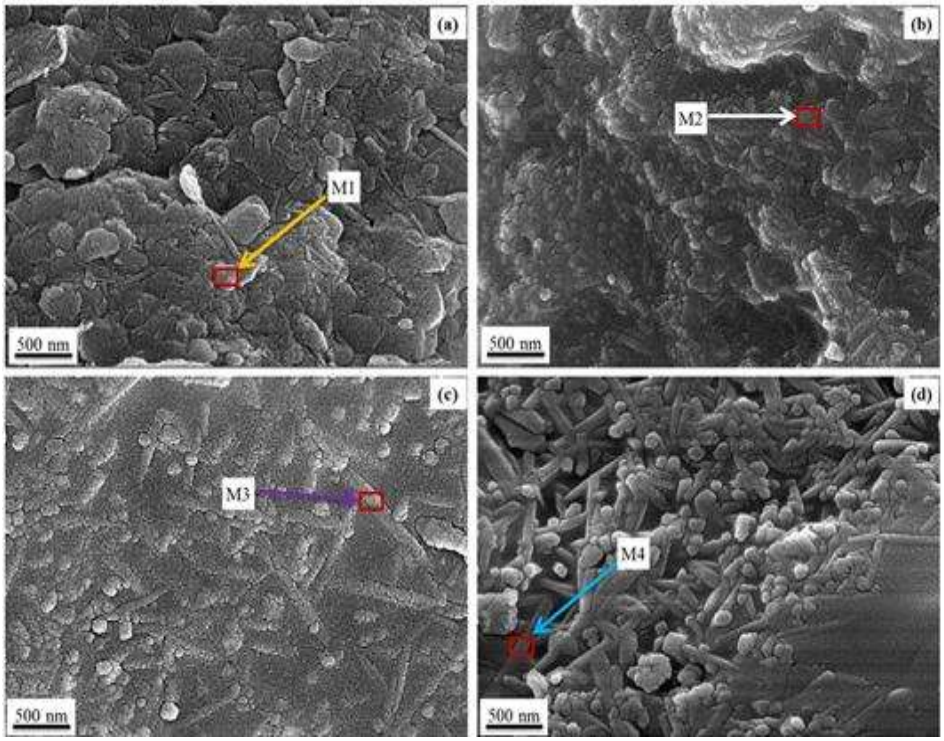

Fig. 4.11: SEM image portraying surface morphology of sample (a) C-1, (b) C-2, (c) C-3, and (d) C-4 sintered at 1200 °C.

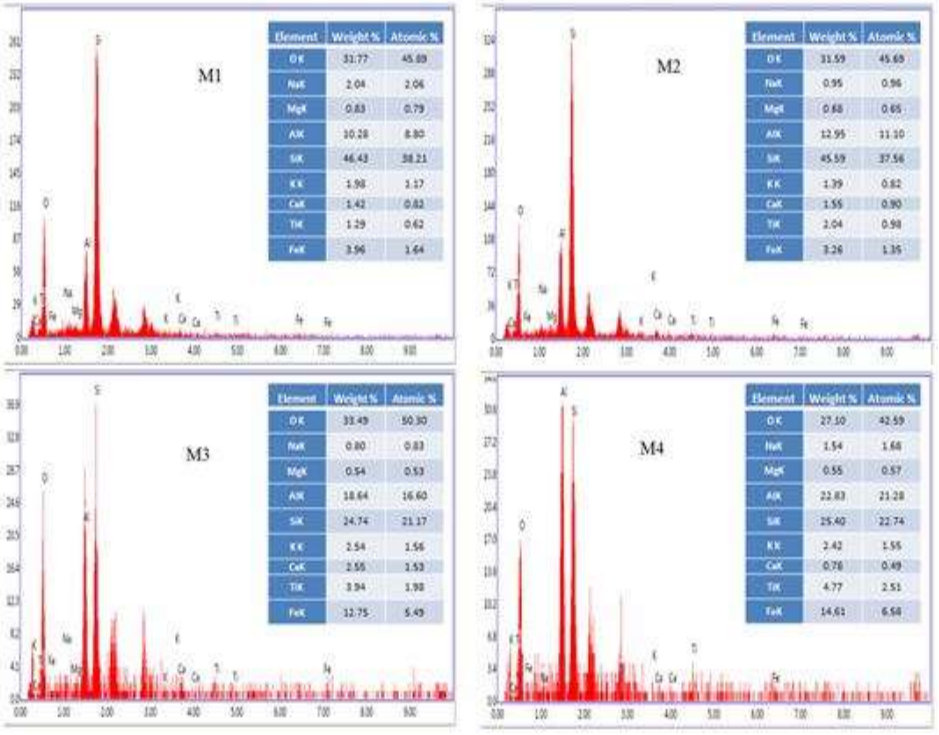

Fig. 4.12: EDS analysis of points M1, M2, M3, and M4 for formulations C-1, C-

2, C-3, and C-4, respectively, as represented in SEM images.

more giant rod-like shape by solution-precipitation, which can be observed from **Fig. 4.11 (a), (b), (c), (d),** and **Fig. 4.13 (a)**[155]. For Fig.4.1(a), irregular round type grain structure along with a small amount of rod-like mullite structure were observed. Comparatively, prominent and large-sized mullite structures started to grow on the SiO_2 matrix, which can be seen from **Fig. 4.11(b)**. **Fig .4.11(c)** shows that formulation C-3 has a large number of elongated in-situ mullite formations, which increased for formulation C-4 (**Fig. 4.11(d)**) with the increasing amount of ball clay content. The elemental

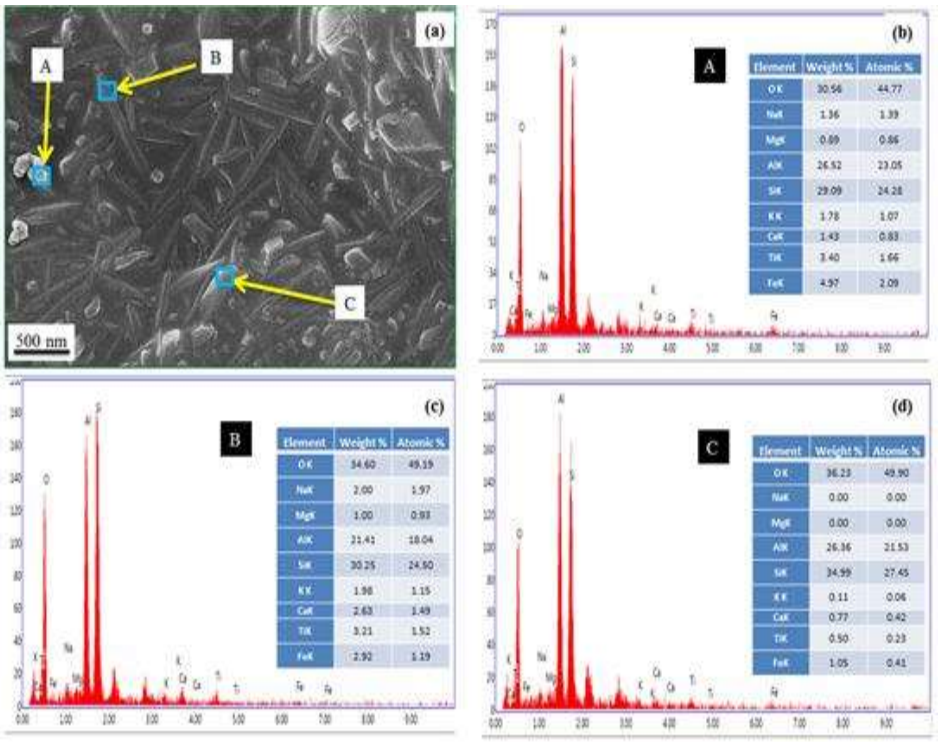

Fig. 4.13: SEM image portraying surface morphology of sample (a) C-5 with EDS analysis sintered at 1200 °C.

composition of points M1, M2, M3 and M4 were analyzed using EDX and represented

in **Fig. 4.12**. The EDX results indicate that the elemental concentrations were within the range of silica-rich mullite compositions. The fired samples were densified as the liquid phase gradually formed, cementing the matrix and reducing fissures and cracks. The flow mechanism (viscous) of the liquid phase encourages the dense organization of mullite grains, cristobalite, and the residual quartz in the matrix. The interlocking of crystals reduced grain boundaries between pores and gaps, which enhances the density and strength [148,149]. SEM image along with EDX analysis of formulation C-5 is shown in **Fig. 4.13 (b), (c), (d)** at different spots (A, B, and C) indicate the right proportion of the existing elements in the fired samples.

4.3 Summary of results

This study successfully established that dense fireclay refractory could be produced using ball clay and lignite fly ash. The addition of ball clay enhances the plasticity of the non-plastic lignite fly ash permitting the bodies to be formed. Varying the ball clay content with lignite fly ash and firing at 1200 °C for 2 hours can improve the properties of the sintered compositions. The total linear shrinkage (firing) was observed less than 5.38%, making it appropriate for refractory material. The apparent porosity and bulk density were achieved 15% and 2.10 gm/cc for C-5 formulation when fired at 1200 °C for 2 hours. On the other hand, the properties such as thermal conductivity, CCS, and CMOR values of the C-5 formulation were superior to the other formulation and well-matched with ASTM standard and commercially available products. The presence of the cristobalite phase, rod-like mullite, and interlocking grain structure confirmed by XRD and SEM analysis were the primary reasons for those enhanced properties. Therefore, the C-5 formulation fired at 1200 °C for 2 hours

can be implemented as a dense fireclay refractory. So, it can be concluded from the investigation that there is a possibility of using lignite fly ash as a raw material for fireclay alumina-silicate refractory. As a result, a significant amount of lignite fly ash produced at a thermal power plant can be reused, which will reduce the cost for special redemption of fly ash and thereby protect the environment. Finally, it can be concluded that the produced fireclay refractory can be used for low to high duty applications in boiler, kiln, and blast furnace.